Probability maps of optic radiation in patients wtih hippocampal sclerosis

I. Mader[1], V. Glauche[2], H. Mast[1], M. Unfried[3], K. A. Il'yasov[4], and B. W. Kreher[4]

[1]Neuroradiology, University Hospital Freiburg, Freiburg, Germany, [2]Neurology, University Hospital Freiburg, Freiburg, Germany, [3]Neurosurgery, University Hospital Freiburg, Freiburg, Germany, [4]Medical Physics, University Hospital Freiburg, Freiburg, Germany

Introduction

Fiber tracking of the optic radiation is often hampered by the strong bending of the Meyer loop or by mis-tracking into the temporal pole, when the FACT algorithm is used. Another problem is the definition of regions of interest, because they have to be created manually in the individual anatomical data set of the patient. The purpose of this study was to overcome the problems of the FACT algorithm by using probability maps, and to create the seed points by a parameterised method.

Methods

Eight patients with hippocampal sclerosis previous to selective amygdalohippocampectomy were investigated by Diffusion Tensor Imaging (DTI) at a 3T whole body system. Parameters of the FLAIR SE EPI sequence were: TR 11.8s, TI 2257ms, TE 96ms, pixel size 2x2x2 mm^3, b-value 1000s/mm^2, and 61 diffusion encoding directions. Geometric distortions were automatically corrected [1]. Offline DTI analysis was performed by an in-house developed DTI and Fibertools Software Package [2] running under Matlab (The Mathworks, USA). For the depiction of the lateral geniculate corpus (CGL) and for the primary visual cortex (V1, Brodman area 17), anatomical maps from the WFU Pick Atlas [3] were normalised onto the b0 images of each individual patient data set by using spm5. These maps were imported into the DTI and Fibertools software [2] and used as seed points. Arising from these four seed points (CGL and V1 on both sides) probability maps were calculated for each optic radiation (www.uniklinik-freiburg.de/mr/live/arbeitsgruppen/diffusion/fibertools_en.html). To achieve a further quantitative evaluation of the found probabilities of the optic radiation, additional ROIs were created as orbitals around each CGL, with a diameter of 10mm, 30mm, and 50mm and a thickness of 20mm each. The first orbital is then resulting in a sphere, Fig. 1. From the cross section of the optic radiation and the orbitals, the calculated probabilities were extracted and pooled into a pathologic side and a healthy side. A log-it transformation according to $P_{log} = P_0/1\text{-}P_0$ was performed to achieve a normal distribution. Additionally, the number of found pixels containing probabilities of optic radiation was also extracted for the pathologic and the healthy side, respectively. A paired t-test was performed.

Results

In all patients, the optic radiation was equally depicted by probability maps in the orbitals nearest to the CGL and nearest to V1 on both sides. Only in the intermediate part (2nd orbital) a significant difference was visible. Here, the probabilities were higher on the pathologic side, Table 1. The numbers of pixels containing the optic radiation was also equal on both sides.

Discussion

The preoperative detection of optic radiation in patients with hippocampal sclerosis is desired to protect this fiber bundle during operation. By using probabilistic maps and automated atlas-based definition of seed points (CGL and V1), the optic radiation in all patients was depicted, Fig. 2**.** As this fiber structure is not expected to change with hippocampal sclerosis, it is somewhat unexpected to find a significant difference of probabilities in the intermediate part of the optic radiation. This might be attributed to volume changes on the pathologic side (increasing side ventricle) and subsequent narrowing of the fiber bundle which may lead to a higher fractional anisotropy. The equal number of found pixels on both sides, however, contradicts this hypothesis, but also indicates a robust means for pre-operative depiction of optic radiation.

References

[1] Zaitsev M. Proc. Intl. Soc. Mag. Reson. Med. 14 (2006) 1024

[2] Kreher B.W. Proc. Intl. Soc. Mag. Reson. Med. 14 (2006) 2758

[3] Maldjian, J.A. NeuroImage 19 (2003) 1233– 1239

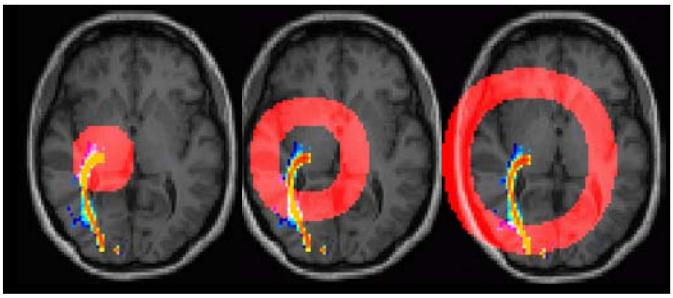

Figure 1
Example for the cross-sections of the optic radiation and the orbitals, from where the probabilities and numbers of found pixels were selected.

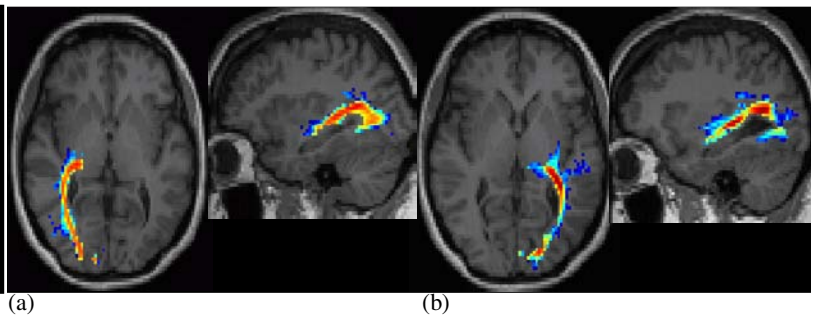

(a) (b)

Figure 2
Example of a probabilistic map of the optic radiation on the side of hippocampal sclerosis (a) and of the healthy side (b). Red colour encodes high, blue low probabilities.

	P_{log} 1rst orbital	Range 1rst orbital	P_{log} 2nd orbital	Range 2nd orbital	P_{log} 3rd orbital	Range 3rrd orbital
Pathological	-18,27	5,42	-21,10*	6,03	-20,59	6,30
Healthy	-18,22	5,53	-21,25*	5,95	-20,65	6,54

Table 1: Means of log transformed relative probabilities and their range
The negative values arise from logarithmic transformation. Only in the intermediate part of the optic radiation (2nd orbital) a higher probability is found on the pathologic side compared to the healthy side, *p = 0.044.